

Field study of film spreading on a sea surface

doi:10.5697/oc.56-3.461
OCEANOLOGIA, 56 (3), 2014.
pp. 461–475.

© Copyright by
Polish Academy of Sciences,
Institute of Oceanology,
2014.

KEYWORDS

Oil slick
Film spreading
Sea surface pollution
Field study

ALEKSANDR E. KORINENKO^{1,*}
VLADIMIR V. MALINOVSKY^{1,2}

¹ Marine Hydrophysical Institute of the NAS of Ukraine,
Kapitanskaya 2, Sevastopol 299011, Ukraine;

e-mail: korinenko.alex@gmail.com

*corresponding author

² Small Enterprise DVS LTD,
Kapitanskaya 4, Sevastopol 299011, Ukraine

Received 20 December 2012, revised 14 March 2014, accepted 31 March 2014.

Abstract

The results of a field study of surface film spreading on the sea surface are presented. The experiments were carried out in the coastal zone of the Black Sea in a wide range of wind speeds and wave conditions. Vegetable oil was used for preparing the surfactants. It was found that at moderate and strong wind speeds the slicks take on a shape similar to an ellipse and are orientated in the direction of the air flow. An increase in the speed of the spreading slick along its major axis with strong wind was discovered.

1. Introduction

An important aspect of the research problem of slicks on a sea surface is the study of their temporal dynamics. One of the significant parameters of surface films (SF) of different origin is their characteristic dimensions. Generally accepted theoretical models discriminate the process of spot

The complete text of the paper is available at <http://www.iopan.gda.pl/oceanologia/>

spreading into typical temporal spreading stages: one or another physical mechanism prevails at each stage.

Fay (1969) identified three consecutive basic stages in the spread of an initially concentrated volume of oil with constant properties, notably, gravity-inertial (balance between gravitational force and inertial force), gravity-viscous (balance between gravitational force and frictional force), and the surface tension regime, when the surface tension force and frictional force are in balance.

These three stages are all characterised by power laws governing the size of the slick as a function of time $\propto t^\beta$ but with different coefficients α and β for each stage. Fay's classification was a powerful incentive for the phased studying of these processes.

A great many research papers are dedicated to theoretical models and laboratory measurements of film spreading (e.g. Hoult 1972, Foda & Cox 1980, Camp & Berg 1987, Dussaud & Troian 1998, Svitova et al. 1999, Boniewicz-Szmyt & Pogorzelski 2008 and references therein).

In particular, Hoult (1972) and Buckmaster (1973) give theoretical analyses for the spread of oil slicks on a quiescent body of water. The dependence of the film border on time, thickness and velocity distributions along a spreading film were analysed in detail by Foda & Cox (1980) and Phillips (1997) for both plane and axisymmetric slicks. Laboratory results of surface film dynamic of various pure oils and their liquid solutions (Camp & Berg 1987) are in good agreement with the model calculations presented by Foda & Cox (1980).

Boniewicz-Szmyt & Pogorzelski (2008) used video-enhanced microscopy and dynamic tensiometry methods to study the spreading of different liquid hydrocarbons in laboratory conditions. According to the experimental observations of these authors, the lens expansion rates are one order of magnitude lower than those predicted by classical tension-gradient-driven spreading theory. These authors proposed a surfactant rate-limited adsorption mechanism to explain the results they obtained.

The investigations mentioned above address the idealised case of a circular film spreading on a 'calm sea'. However, the results of such studies do not describe the asymmetric spreading of surface spots in wind, wave and current fields.

In environmental conditions a surface film elongates and tends towards a shape close to an ellipse (e.g. Lehr et al. 1984a, Elliot 1986). Lehr et al. (1984b) linked the changing size of an oil spill with wind action. These authors proposed an empirical formula to describe the extension of the oil slick in the wind direction as a term that increases in magnitude with time in proportion to the wind speed. Lateral spreading of the oil spill

was described by the formula for the gravity-viscous stage. The important conclusion of the results obtained by Lehr et al. (1984b) is that the spreading rate along the major axis (the derivative of axis length with respect to time) has to increase as the wind strengthens. However, this empirical approach does not explain the physical causes of the asymmetrical spreading of surface pollution.

Elliot (1986) developed the concept of shear spreading caused by the natural dispersion and subsequent resurfacing of oil droplets. In this model the slick size was calculated using the velocity shear for wind and wave conditions observed during the experiment (Elliot 1986). The model predicts that the elongation of a slick will increase with increasing wind speed and wave height.

The validation of oil spill models is complicated owing to the lack of observations in natural conditions, including the simultaneous recording of wind/wave parameters and oil spill dynamics. Field investigations can be resources for estimating the actual impact of wind and waves on SF spreading.

The aim of the present study is to compare film spreading characteristics with wind and sea wave parameters obtained during field experiments.

2. Experimental

2.1. Measurement methods of oil film spreading

The results presented in this paper are based on the field data collected during controlled releases of film slicks in 2005–2007. An investigation of oil spreading was carried out in the vicinity of an oceanographic platform (off the southern coast of Crimea, $44^{\circ}23'35''\text{N}$, $33^{\circ}59'4''\text{E}$), located about 450 m from the shore; the sea depth there is 30 m.

Vegetable oil (VO) was used for the preparation of surfactants. 94–96% of vegetable oil consists of mixtures of insoluble fatty acids; the remainder resembles fats and free fatty components. Vegetable oil forms a film on the water surface and remains uniform at wind speeds up to $10\text{--}12\text{ m s}^{-1}$. This allows film spreading to be investigated in a wide range of meteorological conditions.

Volumes of vegetable oil ($170 \times 10^{-6}\text{ m}^3$ in 2004 and $340 \times 10^{-6}\text{ m}^3$ in 2005–2007) were poured into the water from a motor boat at a distance of 1000–1500 m from the shore; at these distances the water depth exceeds 60 m.

The sea surface area covered with the VO film was registered using a digital camera. Image resolution was 2288×1712 pixels. The camera was placed on a rock at a height of 150 m above the sea level. The distance to

the platform was 1290 m. Each experiment was accompanied by consecutive photography at intervals of 3–4 min from the release of the slicks until its destruction. The photography was done at different camera field of view angles, varying from $6^\circ \times 4.2^\circ$ to $49.1^\circ \times 36.7^\circ$.

The scheme of the experiment is presented in Figure 1, where the oceanographic platform, the camera's position on the rock and the boat's position (conditional) are marked by the symbols P, C and B respectively.

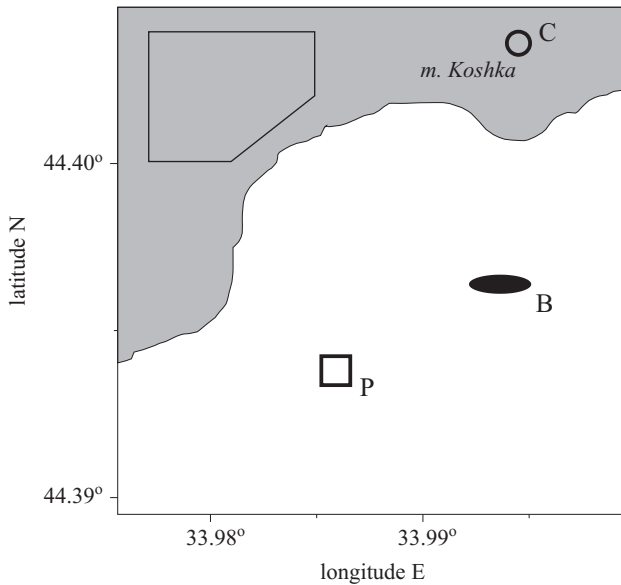


Figure 1. Scheme of the experiment. The symbols P, C and B respectively designate the platform, the camera's position on Mount Koshka and the boat's position

The known geometry of the proving ground enabled the photographs of the sea surface to be converted into a rectangular system of horizontal coordinates. The origins of the coordinates of the converted photographs correspond to the intersection point of the optical axis of the camera's objective with the sea surface.

An example of the vegetable oil film evolution during the measurements carried out on 9 August 2005 (run No. 1) is demonstrated in Figure 2, which shows a series of six converted photos. The images were made at fixed time periods of 240 s, 420 s, 840 s, 1200 s, 1860 s and 1920 s from the beginning of the spillage. The wind direction with the speed of 7.9 m s^{-1} is shown by the arrows in Figure 2.

The slick contour on the sea surface was reconstructed according to the converted images. Then all the coordinate systems of the converted images were converted into the Cartesian coordinate system. This allowed

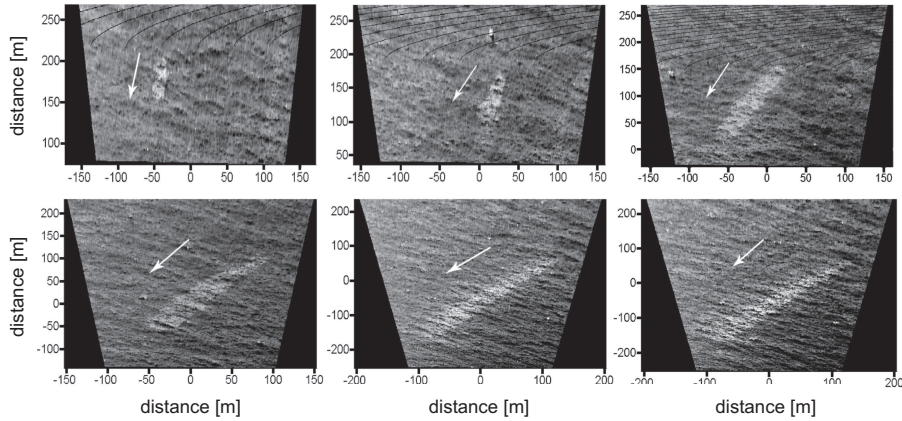


Figure 2. An example of vegetable oil film evolution. The images were taken at fixed times of 240 s, 420 s, 840 s, 1200 s, 1860 s and 1920 s from the start of the spillage. The arrows indicate the direction of the wind

the spatial orientation of the surface slicks to be compared with the wind speed direction.

The sea surface photography was accompanied by hydro-meteorological measurements.

The system for measuring the wind speed U and its direction φ_U , water temperature T_w and air temperature T_a was placed on the oceanographic platform. The wind speed and direction at a horizon of 23 m were measured by meteorological vane anemometer. The instrumental errors of all thermometers were less than $\pm 0.05^\circ$; those of the anemometer were less than $\pm 0.2 \text{ m s}^{-1}$. Recalculation of the wind speed at a standard meteorological horizon of 10 m was carried out by the method proposed by Large & Pond (1981).

The characteristics of surface waves were determined by a resistant wave staff that recorded sea surface elevations in the frequency range $f \leq 1 \text{ Hz}$. The distance from the wave staff to the platform was 9 m.

In accordance with the wave data the significant wave heights $H_s = 4\sigma_\zeta$ (where σ_ζ – standard mean deviation of the surface elevation) were calculated. The frequency spectra of sea surface elevations $S(f)$ were plotted using a standardised technique (Bendat & Piersol 1999).

Table 1 summarises the environmental conditions during the experiments. The date, serial number of the measurement and the mean values of \overline{U} , $\overline{\varphi_U}$, T_a , T_w , H_S are given.

As follows from Table 1 the measurements were carried out in a wide range of wind speeds at neutral atmosphere stratification.

Table 1. Experimental conditions

Date	No. ser.	\bar{U} [m s ⁻¹]	$\overline{\varphi U}$ [deg]	T_a [C°]	T_w [C°]	H_s [m]
23.08.04	2	10.7	254	24.3	25.0	0.32
26.09.04	3	6.3	240	20.7	22.7	0.31
07.08.05	2	1.6	130	28.5	26.5	0.62
08.08.05	1	11.7	246	25.0	24.8	1.03
	2	11.6	248	25.1	24.9	1.00
09.09.05	1	7.9	246	26.3	24.6	0.69
	2	10.2	244	26.4	24.6	0.76
	3	11.6	244	25.4	24.7	0.75
16.08.05	1	7.8	99	26.9	26.1	0.63
	2	9.0	96	27.1	26.0	0.63
24.08.05	1	1.6	174	25.2	26.2	0.20
	3	1.6	191	25.3	26.3	0.20
26.08.05	1	8.1	258	25.3	25.4	0.25
	2	10.6	258	25.4	25.5	0.36
12.08.06	1	3.3	85	26.4	23.5	0.29
15.08.07	1	2.7	102	29.3	26.2	0.15

2.2. Surface tension coefficient measurement

The time interval determining the dynamics of surface films at each of the spreading stages depends on both the properties and the amount of spilled substance (Fay 1969). The inertial stage is the quickest one. For instance, if the amount of poured material is at least 10 m³, the enlargement of the SF radius will last several minutes according to the law $R(t) \sim t^{1/2}$. During the next few hours the slick axis length will grow under the influence of gravitational and viscous forces as $\sim t^{1/4}$. The final stage of spot spreading is the surface tension stage. It is thought that if the amount of poured material is less than 1 m³, the surface tension stage actually occurs from the very beginning of spot spreading. In our experiments the volume of spilled material was no more than 340×10^{-6} m³. Thus we can assume that in fact from the release of the slick the VO film spreads under the forces of surface tension and viscosity.

Spreading at this stage depends on the spreading coefficient (SC), defined as

$$S = \sigma_{wa} - (\sigma_{fa} + \sigma_{fw}),$$

where σ_{wa} , σ_{fw} , σ_{fa} are the coefficients of the interfacial tensions of water-air, water-film and film-air respectively. For spreading to proceed, the condition $S > 0$ must be satisfied.

The values of the coefficients σ_{wa} and water covered with oil film ($\sigma_{fa} + \sigma_{fw}$) were estimated under laboratory conditions.

Standing waves were generated by a mechanical oscillator; they had sinusoidal horizontal oscillations of frequency f in a vessel of size $10 \text{ cm} \times 10 \text{ cm} \times 2 \text{ cm}$ equipped with etalon length markers.

A pattern of bright and dark bands corresponding to the provisions of the crests and troughs of the standing waves in the cell was recorded with a digital camera. The camera was directed vertically downwards. The size of the images was 3888×2592 pixels. The crests of standing waves are parallel along the short side of the picture. Fast Fourier transform was used to calculate the spectrum of brightness for each image row. Then the whole brightness spectrum was averaged and the wave number of the standing waves k_w , corresponding to the maximum value of the spectrum, was determined.

The value of k_w with a known wave frequency allows us to calculate the surface tension coefficient from the dispersion relationship as follows:

$$\sigma = \rho \frac{\omega^2 - gk}{k^3},$$

where $\omega = 2\pi f$ – angular frequency of oscillations, $k = k_m/2$ – wavenumber of surface wave, ρ – water density, g – acceleration due to gravity.

According to the laboratory measurement results, the spreading coefficient for a saturated monolayer of vegetable oil was $S \approx (32 \pm 4) 10^{-3} \text{ N m}^{-1}$. The measurement error of SC was no less than 10%.

3. Results and discussion

During the experiment 16 series of film spreading measurements were obtained under different wave and wind conditions. The wind speed range was from 1.6 to 11.7 m s^{-1} . Significant wave heights varied from 0.15 to 1.03 m .

Slicks have an elongate shape under moderate and strong winds. The semi-major axis and semi-minor axis of the slick are denoted by L and l respectively.

The direction of the semi-major axis of SF with the wind direction is compared in Figure 3. The figure shows that the surface films are stretched in the direction of the air flow. The data obtained are in qualitative agreement with the results of the previous field studies by Lehr et al. (1984a) and Elliot (1986).

An example of the dependence of L in the downwind speed direction and film area S on time is presented in Figure 4. Data obtained at various wind speeds are shown in this figure by the symbols (o) – 1.6 m s^{-1} – 3.3 m s^{-1} ,

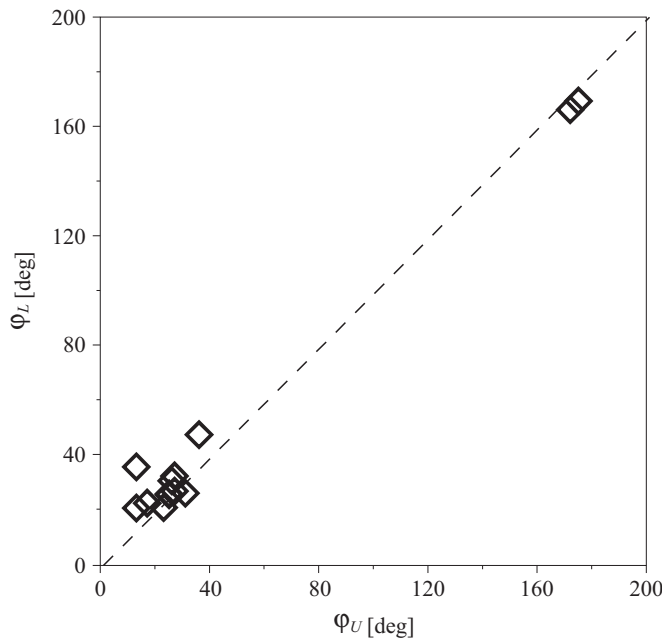


Figure 3. Comparison of the direction the semi-major axis of surface film with the wind direction

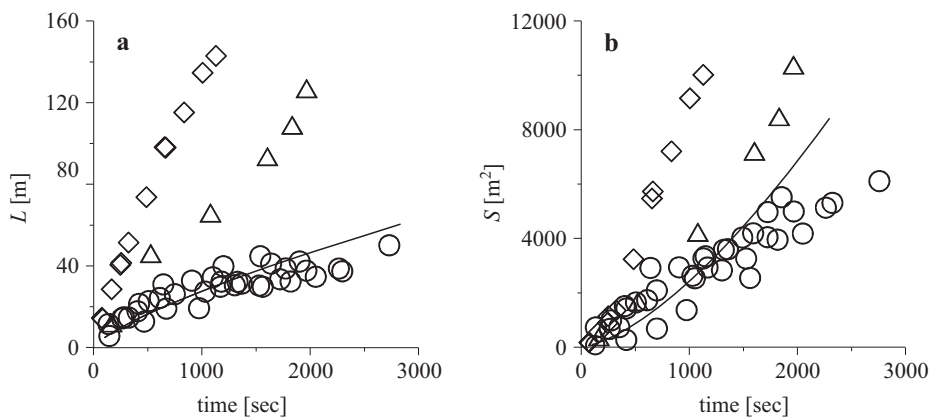


Figure 4. Dependences of surface film sizes on time: a) – radius L , b) – square S . Values measured under different wind speed are marked with (○) – U from 1.6 to 3.6 m s^{-1} , (△) – $U = 7.8 \text{ m s}^{-1}$, (◇) – $U = 11.7 \text{ m s}^{-1}$. The solid line in Figure 4 corresponds to model (1)

(△) – 7.8 m s^{-1} , (◇) – 11.7 m s^{-1} . The origin of the coordinates in Figure 4 corresponds to the moment when the vegetable oil was first spilt. As follows from Figure 4 the values of L at a fixed time point grow when the wind speed

increases. The same tendency is observed for areas of SF (Figure 4 b). We did not find an explicit dependence of the film slick axis l on wind speed.

The values of the ratio L/l describing slick elongation at various times in the wind speed range from 9 to 11.7 m s⁻¹, from 6 to 9 m s⁻¹ and < 3.3 m s⁻¹ are shown in Figure 5 by the symbols (+), (◊) and (○) respectively. The solid line shows the value of $L/l = 1$.

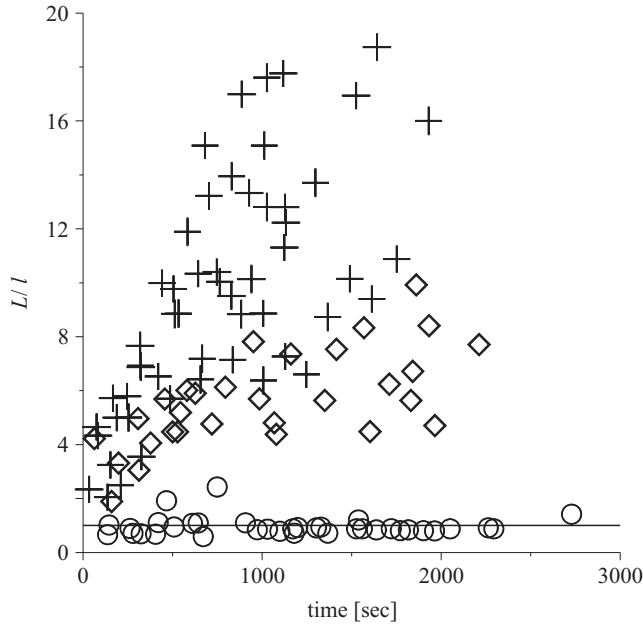


Figure 5. Dependence of the ratio of the large film axis to the small axis on time. Values measured for a wind speed range from 9 to 11.7 m s⁻¹ – (+), from 6 to 9 m s⁻¹ – (◊) and < 3.3 m s⁻¹ – (○). The solid line corresponds to $L/l = 1$

As can be seen from Figure 5 at $U < 3.6$ m s⁻¹ the values of L/l change from 0.9 to 1.1. Thus under calm wind conditions SF is circular in shape. Film slick elongation increases with a strengthening wind and at $U \sim 12$ m s⁻¹ values of L/l are ~ 18 .

Let us define the rate of semi-major axis growth in the downwind and upwind directions as $u_{sp}^d = \partial L^d / \partial t$ and $u_{sp}^{up} = \partial L^{up} / \partial t$ respectively.

Wind speed dependences of spreading rates in the downwind and upwind direction are presented in Figure 6 and denoted by the symbols (○) and (+) accordingly. Values of u_{sp}^{up} and u_{sp}^d were calculated using all the data of each measurement and thus represent average values. Spreading rates at weak wind speeds varied from 0.01 to 0.02 m s⁻¹. There is an increase of values of u_{sp} for moderate and strong winds. According to the results of the experiments, the observed spreading rate of the semi-major axis of the film

at $U = 12 \text{ m s}^{-1}$ is ~ 4 times higher than the value typical of $U = 1.6 \text{ m s}^{-1} - 3.6 \text{ m s}^{-1}$ (see Figure 6).

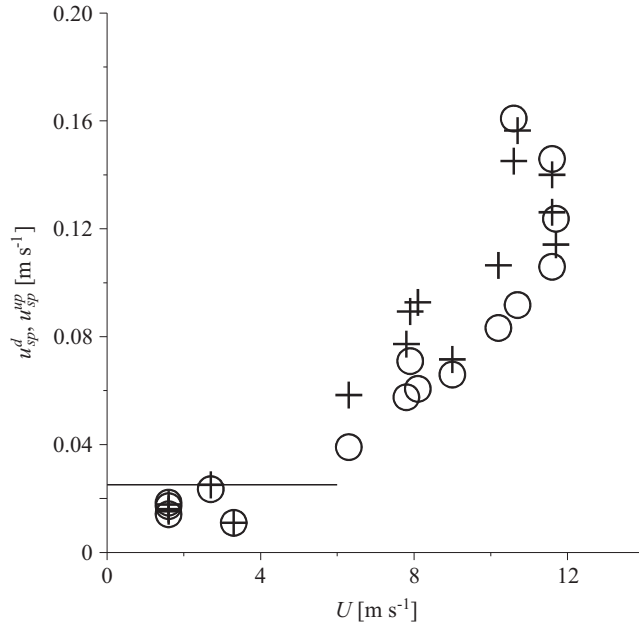


Figure 6. Dependences of mean film spreading rate on wind speed: (o) – along the wind speed direction; (+) – against the wind speed direction. The solid line is the theoretical value estimated using model (2)

Now we consider the growth of the surface film size under various wave conditions. The dependence of u_{sp}^d on H_s is presented in Figure 7, where the symbols correspond to measurements at various inverse wave ages $\alpha = U/C_p$ (C_p – wave phase velocity of the spectral peak): (o) – $\alpha = 0.9-1.3$; (+) – $\alpha = 2-3$. The case denoted by (•) relates to calm wind conditions and to the presence of a swell. As follows from Figure 7, no explicit dependence of the SF spreading rate on H_s for the whole set of points is observed. In contrast, the tendency of u_{sp}^d to increase with increasing wave height for the obtained data set is visible when $\alpha = 0.9-1.3$ and $\alpha = 2-3$. At the same time spreading rates for the case denoted by (•) measured at $H_s = 0.62 \text{ m}$ and $U = 1.6 \text{ m s}^{-1}$ almost coincide with the values of u_{sp}^d measured at $H_s = 0.15-0.3 \text{ m}$.

As noted above, one can expect that from the beginning of spot spreading, the surface tension regime is operative. The change of the film size with time in the absence of wind is determined by the balance of viscosity and surface tension.

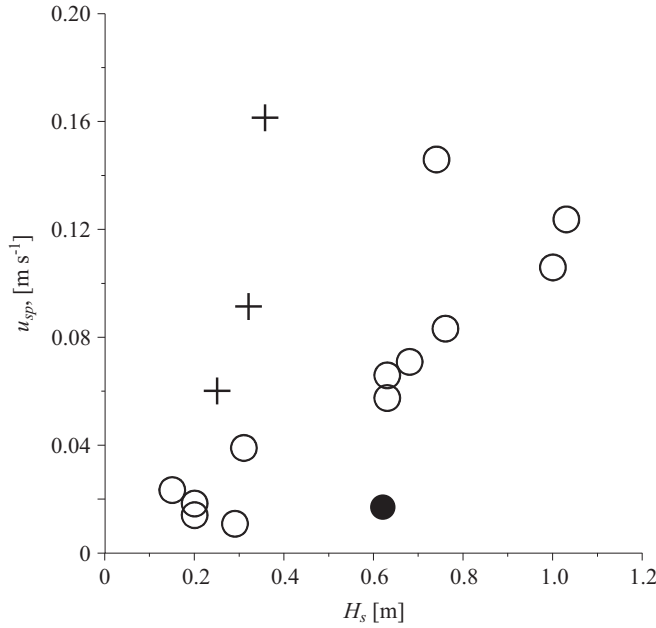


Figure 7. Dependence of the spreading rate on the significant wave height. The symbols correspond to the inverse wave ages: (○) – $\alpha = 0.9 - 1.3$, (+) – $\alpha = 2 - 3$, (●) – calm wind conditions with the presence of swell

The leading edge position and the spreading rate of SF as a function of time t are written as (Fay 1969, Hoult 1972, Foda & Cox 1980, Phillips 1997)

$$R(t) = K \frac{S^{1/2}}{(\mu\rho)^{1/4}} t^{3/4}, \quad (1)$$

$$u_{sp}^0(t) = \frac{\partial R}{\partial t} = \frac{3}{4} K \frac{S^{1/2}}{(\mu\rho)^{1/4}} t^{-1/4}, \quad (2)$$

where μ – kinematic viscosity of water, K – experimental constant that can range in magnitude from 0.665 to 1.52 (Dussaud & Troian 1998).

It was shown by Camp & Berg (1987), Dussaud & Troian (1998) and Foda & Cox (1980) that expression (1) gives a good description of the SF spreading of various substances under laboratory conditions. The values of u_{sp} shown in Figures 6 and 7 were averaged over the duration of each measurement. To compare our data with model (2) the value of $\overline{u_{sp}^0}$ was calculated in the temporal interval from 200 sec to 3600 sec.

Let us now consider the spreading of a vegetable oil film on the sea surface at a weak wind speed. As can be seen from Figure 4, the spreading of slicks at weak wind speeds (symbols (○) in Figure 4) in fact obeys

the law $R(t) \sim t^{3/4}$ and $S(t) \sim t^{3/2}$ over a significant time interval. The essential difference between the model and experimental data is observed after sufficiently long times. As indicated in Boniewicz-Szmyt & Pogorzelski (2008) surfactant adsorption at the air-water and oil-water interfaces could be a possible mechanism for the difference between lens expansion rates of the field data and the classical tension-gradient-driven spreading theory.

Under calm winds the ratio L/l is close to unity (see Figure 5), i.e. the slick is practically round for the duration of the measurement. Thus the dynamics of SF in natural conditions at weak wind speeds is practically completely defined by the spreading coefficient.

At present the problem of the influence of waves and wind on the spreading of surface films is insufficiently studied.

Below we will analyse one specific case observed in the experiment in more detail in order to obtain accurate information about the impact of swell on surface film dynamics.

This case, dated 7 July 2005, was characterised by a stable moderate wind (9 m s^{-1}) blowing until 11:00 hrs, as shown in Figure 8a. Between 11:00 and 11:40 hrs the wind abated to 1.6 m s^{-1} . Surface film spreading was recorded from 11:50 to 12:20 hrs. The observation interval is shown by the arrows in Figure 8a.

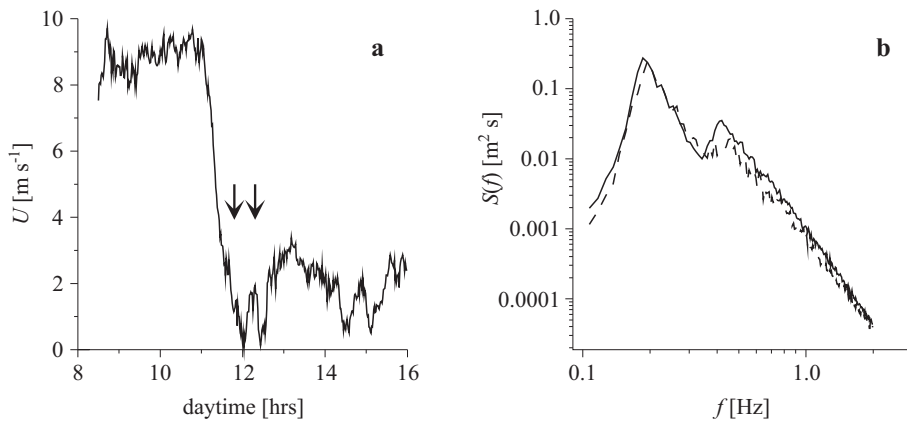


Figure 8. Hydrometeorological parameters from 7 July 2005: a) – wind speed; b) – wind wave frequency spectrum measured during the experiment setup

The wave spectra $S(f)$ measured from 10:00 to 11:00 hrs and from 11:50 to 12:20 hrs are shown in Figure 8b by solid and dashed lines respectively. It can be seen from Figure 8b that the levels of both spectra lie within the frequency range shown. The significant wave heights before and during the experiment were 0.64 and 0.62 m respectively.

Thus, the measured value of the SF spreading rate shown in Figure 7 with symbol (\bullet) was obtained practically in the absence of any wind but in the presence of swell. However, the values of both $L/l = 0.9$ and $u_{sp}^d = 0.017 \text{ m s}^{-1}$ are typical of calm conditions. Moreover, in this case u_{sp}^d is close to the model value of $\overline{u_{sp}^0} = 0.025 \text{ m s}^{-1}$, when the spreading rate is defined only by the spreading coefficients. The fact that the slick shape is nearly circular during the above measurement is confirmed by Figure 9. This shows a photograph of the sea surface, converted into the horizontal Cartesian coordinate system, obtained 2100 sec after the spill. The location of the slick in Figure 9 is indicated by the arrow.

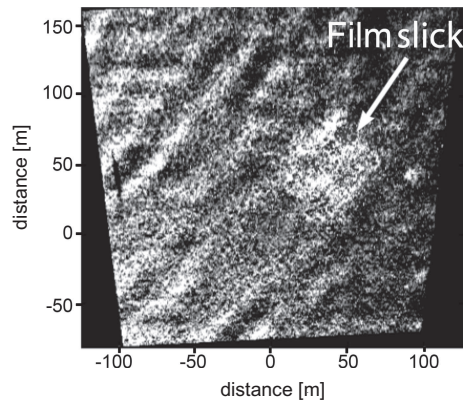


Figure 9. The photographs of the sea surface from 7 July 2005 converted into the horizontal Cartesian coordinate system. The arrow indicates the film slick 2100 s after the spillage

We estimated the wind wave action on SF spreading using frequency spectra at $f \leq 1 \text{ Hz}$. The calculation of $S(f)$ at $f > 1 \text{ Hz}$ is not correct owing to the distortion associated with short-wave advection in the field of long-wave orbital velocities. The influence of the high-frequency part of $S(f)$ on SF spreading will require further study.

4. Conclusion

The investigations of the dynamics of a vegetable oil film on the sea surface were carried out in the vicinity of the Marine Hydrophysical Institute's research platform (off the southern coast of Crimea, $44^{\circ}23'35''\text{N}$, $33^{\circ}59'4''\text{E}$) under a wide range of wind speeds and wave conditions. Slick sizes were estimated from photographic images of the sea surface covered by the surface film.

Analysis of the experimental results showed that the behaviour of the surface film varies, depending on the wind conditions. Film spots tended to become elongate in the direction of the wind flow, taking the form of an ellipse. The rate of semi-major axis growth increases from 0.039 to 0.145 m s⁻¹ when U increases from 6.3 to 11.7 m s⁻¹. In the experiments carried out at wind speeds less than 4 m s⁻¹ and a significant time interval, the law $L \sim t^{3/4}$ was obeyed. According to Fay's classification this corresponds to the spreading mode of the dominant forces of surface tension.

The experimental results show the absence of an explicit dependence of significant wave height from 0.15 to 1.03 m on film spreading rate.

The values of the spreading rates obtained at a weak wind of 1.6 m s⁻¹ but different values of the significant wave heights ($H_s = 0.62$ and $H_s = 0.15$ m) are practically the same.

Acknowledgements

The research leading to these results received funding from the European Community's Seventh Framework Programme (FP7/2007-2013) under Grant Agreement No. 287844 for the project 'Towards Coast to Coast NETWORKS of marine protected areas (from the shore to the high and deep sea), coupled with sea-based wind energy potential (CoCoNET)'. Financial support was also received from IFREMER (Contracts Nos. 2011 2 20712376 and 2012 2 20712805 between IFREMER and Small enterprise DVS LTD).

References

- Bendat J.S., Piersol A.G., 1999, *Random data analysis and measurement procedures*, Wiley, New York, 594 pp.
- Boniewicz-Szmyt K., Pogorzelski S.J., 2008, *Crude oil derivatives on sea water: signatures of spreading dynamics*, J. Marine Syst., 74 (Supp.), 41–51, <http://dx.doi.org/10.1016/j.jmarsys.2007.11.015>.
- Buckmaster J., 1973, *Viscous-gravity spreading of an oil slick*, J. Fluid Mech., 59 (3), 481–491, <http://dx.doi.org/10.1017/S0022112073001667>.
- Camp D.W., Berg J.C., 1987, *The spreading of oil on the water in the surface-tension regime*, J. Fluid Mech., 184, 445–462, <http://dx.doi.org/10.1017/S0022112087002969>.
- Dussaud A.D., Troian S.M., 1998, *Dynamics of spontaneous spreading with evaporation on a deep fluid layer*, Phys. Fluids, 10 (1), 23–38, <http://dx.doi.org/10.1063/1.869546>.
- Elliott A.J., 1986, *Shear diffusion and the spread of oil in the surface layers of the North Sea*, Ocean Dynam., 39 (3), 113–137.

- Fay J. A., 1969, *The spread of oil slicks on a calm sea*, [in:] *Oil on the sea*, D. Hoult (ed.), Plenum, New York, 114 pp.
- Foda M., Cox R. G., 1980, *The spreading of thin liquid films on a water-air interface*, *J. Fluid Mech.*, 101, 33–51, <http://dx.doi.org/10.1017/S0022112080001516>.
- Hoult D., 1972, *Oil spreading on the sea*, *Annu. Rev. Fluid Mech.*, 4, 341–368, <http://dx.doi.org/10.1146/annurev.fl.04.010172.002013>.
- Large W. G., Pond S., 1981, *Open ocean momentum flux measurements in moderate to strong winds*, *J. Phys. Oceanogr.*, 11 (3), 324–336, [http://dx.doi.org/10.1175/1520-0485\(1981\)011<0324:OOMFMI>2.0.CO;2](http://dx.doi.org/10.1175/1520-0485(1981)011<0324:OOMFMI>2.0.CO;2).
- Lehr W. J., Cekirge H. M., Fraga R. J., Belen M. S., 1984a, *Empirical studies of the spreading of oil spills*, *Oil Petrochem. Pollut.*, 2 (1), 7–12, [http://dx.doi.org/10.1016/S0143-7127\(84\)90637-9](http://dx.doi.org/10.1016/S0143-7127(84)90637-9).
- Lehr W. J., Fraga R. J., Belen M. S., Cekirge H. M., 1984b, *A new technique to estimate initial spill size using a modified Fay-type spreading formula*, *Mar. Pollut. Bull.*, 15 (9), 326–329, [http://dx.doi.org/10.1016/0025-326X\(84\)90488-0](http://dx.doi.org/10.1016/0025-326X(84)90488-0).
- Phillips W. R. C., 1997, *On the spreading radius of surface tension driven oil on deep water*, *Appl. Sci. Res.*, 57 (1), 67–80, <http://dx.doi.org/10.1007/BF02528764>.
- Svitova T. F., Hill R. M., Radke C. J., 1999, *Spreading of aqueous dimethyl-didodecylammonium bromide surfactant droplets over liquid hydrocarbon substrates*, *Langmuir*, 15 (21), 7392–7402, <http://dx.doi.org/10.1021/la981683n>.